since 1961

Baltica
http://www.geo.lt/geo/index.php?id=71C

BALTICA Volume 24 Number 2 December 2011 : 61–70

On recent geodynamics of the Eastern Baltic Sea region

Bela Assinovskaya, Juri Shchukin, Victor Gorshkov, Natalia Shcherbakova

Assinovskaya, B., Shchukin, J., Gorshkov V., Shcherbakova, N., 2011. On recent geodynamics of the Eastern Baltic Sea region. *Baltica, 24 (2),* 61–70. Vilnius. ISSN 0067–3064.

Abstract Seismic hazards in the Eastern Baltic region are traditionally considered quite low in frequency or intensity; therefore, seismic data alone do not provide sufficient constraints on the geodynamic models of this region. However, geological and geophysical data can be used to augment seismic data. This paper analyses GPS-based regional crustal motions, strains, and co-seismic deformations to develop geodynamic models for two Baltic Sea regions (Lake Ladoga –Gulf of Finland and Kaliningrad) in this area. These data and earthquake focal mechanisms provided for the Lake Ladoga, Gulf of Finland, and Kaliningrad earthquakes may be useful for the "Seismic Hazard Harmonization in Europe" (SHARE) project, which is devoted to updating seismic hazard models throughout Europe.

Keywords *Geodynamics • Seismicity • Earthquakes • Strain field • Kaliningrad earthquake • Eastern Baltic Sea*

Bela Assinovskaya [belaa@gao.spb.ru], Central Astronomical Observatory RAS at Pulkovo, Pulkovskoye shosse, 65, Saint-Petersburg, Russia; Juri Shchukin [schuk@idg.chph.ras.ru], Institute of Geosphere Dynamics RAS, Leninsky prospect, 38/1, Moscow, Russia; Victor Gorshkov [vigor@gao.spb.ru], Central Astronomical Observatory RAS at Pulkovo, Pulkovskoye shosse, 65, Saint-Petersburg, Russia; Natalia Shcherbakova [coper@gao.spb.ru], Central Astronomical Observatory RAS at Pulkovo, Pulkovskoye shosse, 65, Saint-Petersburg, Russia. *Revised manuscript submitted 22 June 2011; accepted 20 August 2011.*

INTRODUCTION

Geodynamics is a section of geophysics that studies the forces and processes causing large–scale motion and deformation within the crust and mantle of the Earth. The tools associated with geodynamical research include Global Positioning System (GPS), Interferometric Synthetic Aperture Radar (InSAR), and seismic data as well as numerical modelling of recent changes of the Earth's lithosphere. In this study the geodynamics of two areas of the Baltic Sea region is examined using GPS observations (to date the region has a large number of GPS stations) and seismicity data.

Geodynamic research in the Baltic Sea region has been carried out as a part of the BIFROST project (Baseline Inferences for Fennoscandian Rebound Observations, Sea Level, and Tectonics) since 1993. The primary goal of this project is to establish a new three-dimensional (3-D) model of crustal movements based on Global Navigation Satellite Systems (GNSS) observations. The velocity field for Fennoscandia (Fig. 1) was derived from 13 years of data at more than 80 permanent GPS sites (Lidberg *et al.* 2010). Their solutions had a mean internal accuracy of 0.2 mm/year (1-σ) for horizontal velocities**.**

Traditional interpretations of the BIFROST data are modelled in terms of Fennoscandian Glacial Isostatic Adjustment (GIA) (Wu, Johnston, Lambeck 1999; Fjeldskaar *et al.* 2000; Lidberg *et al.* 2010; Scherneck *et al.* 2010; Pascal *et al.* 2010) rather than horizontal deformation geodynamics. This paper will consider horizontal geodynamic models for data in the eastern extent of Fig. 1.

The two strongest earthquakes in the Kaliningrad area occurred in the Baltic Sea (54.88° N, 20.05° E) on September 21, 2004. These M_W~5 events have been well studied both seismically and geologically (Wiejacz 2004; Gregersen *et al.* 2007; Assinovskaya, Ovsov 2008; Grünthal *et al.* 2008*;* Nikolaev 2009). It should be noted that there are deviating opinions on the locations of the Kaliningrad earthquakes, for

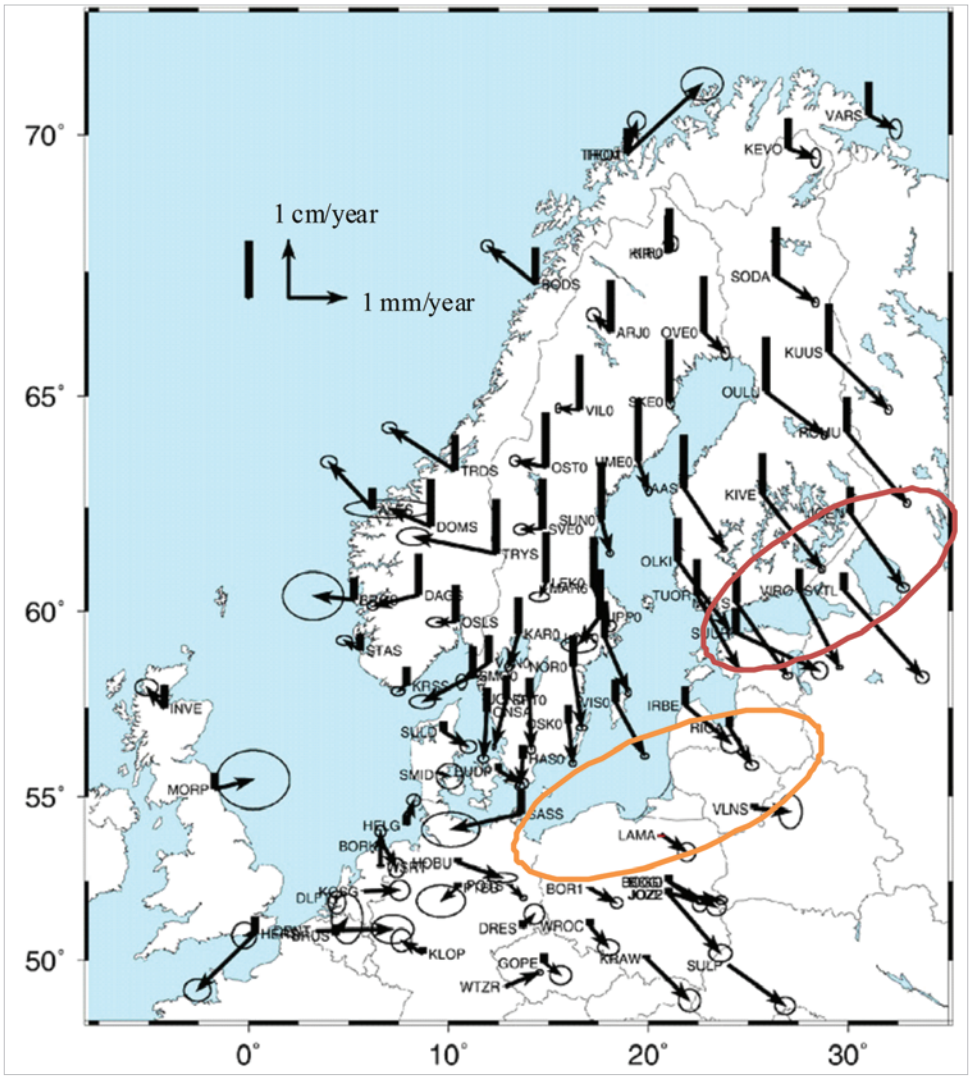

Fig. 1 3–D rates of recent movements in Fennoscandia according to Lidberg *et al.* (2010, Fig. 4) and two regions of this research, Lake Ladoga–Gulf of Finland and the Southern Baltic area around the Kaliningrad earthquake epicentres. After Lidberg *et al.* (2010).

example Nikonov (2006), but in this paper we follow the results of our research (Assinovskaya, Ovsov 2008; Nikolaev 2009).

There is little evidence of seismic activity during the centuries preceding the 21 September 2004 earthquakes, which makes an analysis of the surface and deep strains that resulted from the seismic process interesting in itself. Authors combine geodynamical (GPS) and seismic data to model potential deformations in the region Lake Ladoga–Gulf of Finland and co-seismic deformations in the near–field and far–field zones of the Kaliningrad earthquakes. In both cases, our research is focused on the problem of how tectonic deformation spread throughout these regions and is largely constrained by GPS measurements, earthquake data, and radiation patterns.

DATA AND METHODS

In addition to the BIFROST project data, GPS station motions and earthquake focal mechanisms are used to construct a model of the stress-strain regime in the eastern Baltic Sea region. Since 2008 a permanent GPS monitoring station at the Astronomical Observatory Pulkovo (PULK) has been part of the international European network (Shcherbakova, Gorshkov 2007). However, regular GPS observations have been acquired since 2002. Field GPS observations at the geodetic marks BOTS, GIRS, MELO, and VALM performed by the Institute of Earth Physics of the Russian Academy of Sciences (RAS) during the summer seasons 1999–2008 were also used. Other GPS data for the Lake Ladoga–Gulf of Finland region were collected at the permanent GPS stations JOEN, METS, SUUR, SVTL, and TOIL in 1999–2009. GPS data from the VIRO station were kindly provided by the Finnish Geodetic Institute.

In the Southern Baltic Sea region GPS data were acquired from the permanent stations LAMA, ONSA, RIGA, SPT0, VLNS, WARN, and WLAD. These data were collected from international archive sites (GPS archive 2010) for 2003–2005, also covering the 21 September 2004 Kaliningrad earthquakes (Assinovskaya, Shcherbakova 2010). A daily position for each station was obtained from the GIPSY (GPS Inferred Positioning System) software version 5.0 developed at the Jet Propulsion Laboratory. Final results were transformed to the International GPS Service 2005 (IGS05) reference frame. Incomplete daily data as well as the positions with errors exceeding 3σ were excluded.

Atmospheric loading corrections were added for the Lake Ladoga area GPS series (field and permanent stations) by interpolating appropriate data (Petrov, Boy 2004). These corrections reached ±20 mm in the vertical and 1–4 mm in the horizontal components of the station positions. Hydrological loading corrections for the area were also incorporated into the analysis as this region is close to Lake Ladoga which has large inter–annual variations of the water level (±1 m

and more). These corrections were calculated by J.-P. Boy and were comparable with atmospheric ones. The input variations of the Lake Ladoga water level were taken from satellite altimeter data (Altimeter data 2010).

The location of all GPS stations and geodetic marks are seen in Figures 1, 2, and their positions and annual velocities are presented in Table 1. Low-frequency trends were removed from position time series for Southern Baltic GPS stations surrounding the Kaliningrad earthquake zone. The residuals were examined aiming to determine the offset (step function) in each station position around the day of the Kaliningrad earthquakes. The applied method of shift isolation in GPS time series is close to that used by Wdowinski *et al. (1997*).

The horizontal velocity field of Lake Ladoga–Gulf of Finland GPS stations allows assessment of the deformation pattern after removing

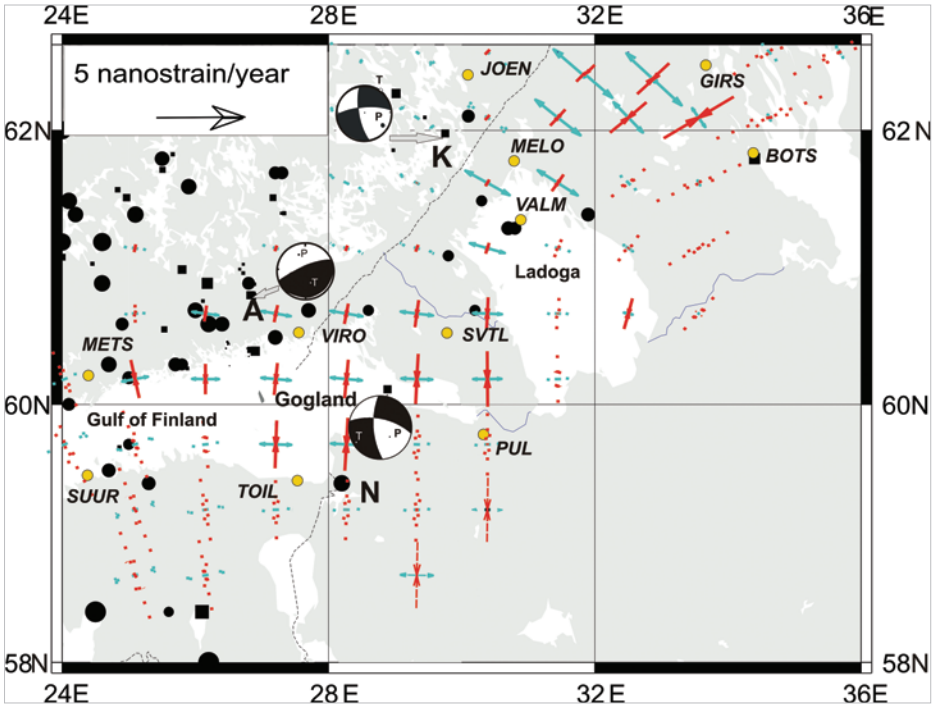

Fig. 2 Strain field ΔL/L (nanostrain/yr) evaluated by GRID_STRAIN software and seismicity around the Lake Ladoga–Gulf of Finland region. Blue arrows represent dilatation and red arrows compression. Strains are calculated on the 50x50 km grid. Solid lines show significant and dotted lines mean significant strain rates. The focal mechanisms for Kesälahti (K), Ananjlankoski (A), and the Gulf of Finland (F) earthquakes are shown. The black area of circles indicates the compression zone and the white area the dilatation zone. Grey arrows connect epicentres with their focal mechanism. Small black circles and squares denote locations of historical and instrumental earthquakes (magnitude ML range 0.1–4.0), respectively, the size of the circles is proportional to the magnitude. "N" shows the location of the 1881 Narva earthquake. Yellow circles represent GPS stations.

Table 1 GPS station positions and average velocities to the north (V_N), east (V_E), and vertical (V_U) derived from observations from 2002 until 2010. Rows shaded in grey show velocity data from Panafidina, Malkin (2006).

Name, country	Lat (N°)	Lon (E°)	Time span	V_N (mm/y)	V_E (mm/y)	V_U (mm/y)
BOTS, Russia	61.842	34.381	1999–2009	10.72±0.16	20.31±0.17	1.44±0.38
GIRS, Russia	62.458	33.667	2001–2009	10.00±0.20	22.28±0.31	5.61±0.79
JOEN, Finland	62.391	30.096	1999–2010	11.71±0.02	20.35±0.02	4.17±0.06
LAMA, Poland	53.892	20.670	2003–2005	12.7±0.1	20.7±0.1	-0.2±0.1
MELO, Russia	61.783	30.785	1999–2009	10.26±0.15	21.91±0.26	4.24±0.39
METS, Finland	60.218	24.395	1999–2010	12.54±0.02	19.79±0.02	4.94±0.04
ONSA, Sweden	57.395	11.926	2003–2005	13.5±0.1	17.8±0.1	2.1±0.1
PULK, Russia	59.772	30.328	2002–2010	11.78±0.02	21.34±0.02	1.48±0.06
RIGA, Latvia	56.949	24.059	2003–2005	12.1±0.1	21.1±0.1	0.4±0.1
SPT0, Sweden	57.715	12.891	2003–2005	13.2±0.1	17.9±0.2	4.2±0.4
SUUR, Estonia	59.464	24.380	2007–2010	12.97±0.10	18.91±0.11	7.63±0.25
SVTL, Russia	60.533	29.781	2006–2010	10.81±0.06	21.13±0.06	2.71±0.16
TOIL, Estonia	59.422	27.536	2008–2010	12.43 0.14	20.87±0.14	3.90±0.31
VALM, Russia	61.360	30.886	1999–2009	10.89±0.14	22.47±0.31	3.29±0.42
VIRO, Finland	60.539	27.555	1999–2007	11.90±0.14	19.95±0.16	3.95±0.36
VIS0, Sweden	57.653	18.367	2003–2005	13.0±0.1	19.5±0.1	2.9±0.1
VLNS, Lithuania	54.653	25.299	2003–2005	12.3±0.1	21.8±0.3	-0.4±0.4
WARN, Germany	54.170	12.101	2003–2005	16.14±0.14	17.46±0.14	6.29±0.34
WLAD, Poland	54.797	18.419	2003–2005	14.10±0.14	18.55±0.16	0.77±0.24

the ITRF2005 (International Terrestrial Reference Frame 2005) absolute rotation pole for Eurasia. GRID_STRAIN software (Teza *et al.* 2007) was used for this. This software presents the strain field as a set of the principal components of the strain calculated on a regular grid. The grid scale has to be comparable to the mean baseline between stations for reliability of strain estimation. The scaling parameter $exp(d(n)/d\theta)$ was used in the GRID_STRAIN software implementation for this purpose, where $d(n)$ is distance between the n-th GPS station and the selected grid node, and $d\theta$ is proposed by the software and is adjustable by a user scale factor. Thereby only the stations closer than $d\theta$ to the selected grid point give a significant contribution to the strain estimate in this node.

The next criterion for significance evaluation is implemented in GRID_STRAIN. The grid plane is subdivided into three equal sectors centered on each grid node. The result is considered highly significant (solid lines on Fig. 2) if at least one GPS station to grid node distance is less than $d\theta$ for each sector. If only two sectors contain a GPS station satisfying this condition, the result is considered mean significant (dashed lines in Fig. 2). No significance can be assigned to the result in the remaining cases.

The seismic data indicate considerable activity in the Baltic Sea region (Ahjos, Uski 1992) in the past 10 years, with the 2004 Kaliningrad events as the largest in the region in the past 300 years (Avotinia *et al.* 1998; Pagaczewski 1972). Earthquake catalogues and databases for this region (Ahjos, Uski 1992; Assinovskaya 2005; Uski *et al.* 2003, 2006) were searched for source locations and focal depths, and magnitudes and origin times, in order to survey the deformation in this area. In addition, two regional permanent seismic stations, installed on Valaam Island and in Vyborg in 2006 (Karpinsky *et al.* 2006), provided additional data to investigate the seismic activity in the Lake Ladoga–Gulf of Finland region.

Geodynamic analyses of focal mechanism solutions for the 1981 Kesälahti earthquake, the Ananjlankoski swarm (2003) of 17 earthquakes, and the Kaliningrad earthquakes of September 21, 2004 are presented in Tables 2 and 3. The parameters of the 2007 earthquake and their focal mechanism were directly determined using broadband and short–period seismograms from the permanent seismic stations in the distance range of 70–463 km (VYB, VAL, VJF, VSU, MEF, KAF, KEF, SUF, JOF, KJN ,VAF, RAF, SRPE, OUL, MSF, KU6).

The dynamics assessment of the Kaliningrad earthquakes was carried out with COULOMB 3.1 software (2010) (see Lin and Stein, 2004; Toda *et al.* 2005), which calculates static displacements and strains caused by fault slip at any surface and at any depth. COULOMB 3.1 also determines Coulomb stress changes across mapped faults and earthquake nodal planes, assuming a model with an elastic half–space and uniform isotropic elastic properties. The COULOMB 3.1 software allows obtaining quantitative strain parameters in contrast to regular focal mechanism analysis.

RESULTS AND DISCUSSION

Lake Ladoga–Gulf of Finland region

Strain rates for the northern Lake Ladoga and eastern Gulf of Finland area are shown in Fig. 2. Four uniform strain zones are apparent. The first zone of uniform strain is the Lake Ladoga–Lake Onega area with largely unaxial compression. The second is the area north of Lake Ladoga which has a motion that is largely uniaxial dilatation with a NW direction coinciding with the stretch of the Lake Ladoga graben long axis (stations MELO – JOEN). The third region includes the Karelian Isthmus (SVTL – PULK) and the Gulf of Finland (VIRO – TOIL and SUUR – METS) and shows approximately equal compressional and tensional strain rates with a deformation pattern in the NS–EW direction (NS – compression, EW – dilatation). Further westward the strain field changes to predominantly compressive. The fourth area, the northern coast of the Gulf, shows motion with EW dilatation. Unfortunately, there are not enough GPS data to extend strain calculations farther to the north where notable seismic activity is present**.**

The borders between these regions may be connected with faulting associated with the development of the Lake Ladoga graben structure that divides blocks of various strain regimes. This stress field may be responsible for crust instability and for earthquake occurrence in this area. The Lake Ladoga–Gulf of Finland region shows a consistent pattern of low magnitude seismicity (Ahjos, Uski 1992; FENCAT database 2010). Epicentres of 42 historical events with magnitudes M_L 1.2–4.0 and focal depths 5–12 km as well as 39 recorded events from 1956 to April 2009 with M_L 0.1–3.5, focal depths 5–10 km are shown in Fig. 2.

16 earthquakes have occurred in the Lake Ladoga region in the past 55 years. Ten of them belong to the Valaam group clustered around the central part of Lake Ladoga (Assinovskaya 2005) and six earthquakes had epicentres along the periphery of the lake (see Fig. 2) as reported by Renquist (1931) and (Nikonov 2005). The comparison of the epicentre locations with local geologic data strongly suggests that all of these earthquakes are connected with the fault system associated with the Lake Ladoga graben. The 2010 Valaam micro–earthquake swarm in fact had tectonic origin.

In addition, five earthquakes with magnitudes M_L 2.3–2.6, focal depths 5–10 km located northwest of the Lake Ladoga structure were recorded between 1979 and 2009 (FENCAT database 2010). The 1981 Kesälahti earthquake (M_L = 2.1) focal mechanism shows strike-slip motion along one of the two NS or EW

trending fault planes, with a NW trend of maximum compression and a S–SW trend of maximum dilatation (Uski *et al.* 2003).

13 historical earthquakes and another 30 recorded instrumentally have occurred close to the northern coast of the Gulf of Finland (see Fig. 2). The 2003 Anjalankoski swarm of micro–earthquakes is included in this amount (Uski *et al.* 2006). The 16 earthquakes (M_L = 0.6–2.1) associated with the Anjalankoski event had focal depths less than 2 km and occurred on the northern shore of the Gulf of Finland. This swarm belongs both to the NE and the ENE–WSW oriented fault zones (Uski *et al.* 2006). The focal mechanism exhibited dip–slip motion on a vertical fault plane with strike 250º, which coincides with the boundary of the Vyborg rapakivi granite batholith. Note that the compressional, P (strike 340º, plunge 35º) and dilatational, T (strike 340º, plunge 55º) axes decline from the horizontal.

The 1881 Narva earthquake epicenter is located on the southern shore of the Gulf. This event is the strongest in this part of the study area and reached the intensity I_0 = VI. The earthquake magnitude and focal depth assessed according to macroseismic data equal M = 3.0 and 5 km, respectively (Ahjos, Uski 1992). The isoseismals extend along the coast of the Gulf. The NW–SE orientation of the Narva–Anjalankoski seismic activity zone probably extends into eastern Gulf of Finland. This is indicated by the existence of palaeo–seismic deformation found on Gogland Island in the central part of the Gulf. This island is located between the Narva 1881 earthquake epicentre on the southern coast of the Gulf and the epicentre cluster of the Anjalankoski earthquakes on its NW side (Assinovskaya, Verzilin 2007).

The 2007 event in the eastern section of the Gulf of Finland (see Fig. 2) had M_L 2.0 and depth 2.9 km. The focal mechanism solution yielded possible fault planes in the NS and NW–SE directions, respectively. The latter orientation coincides with that of the basement faults revealed by Amantov *et al.* (2002) and is therefore preferred (see Fig. 2). The best fitting dynamics for this focal mechanism would include strike–slip and normal motion along a NW–SE fault line with NW–SE orientated maximum compression and NE–SW oriented maximum dilatation. Note that the dilatation axis is close to the horizontal (T-axis strike 230º, plunge 3º; P-axis strike 317º, plunge 41º).

Thus, the weak seismicity of the northern Lake Ladoga area is connected with the surface geodynamic dilatation zone as well as with the strain change boundaries. This deformation style differs from that derived from the 1981 earthquake focal mechanism data. The mainly strike–slip focal mechanism implies a change in the strain regime at a depth of 10 km from the NW trending compression observed by GPS measurements at the surface. GPS observations give satisfactory estimates of surface strain rates, but they are not capable to provide the same quality at depth. Probably, a temporal change in stress is connected with the seismic process, but it is impossible to state this definitely, since the earthquake happened in 1981 and the GPS data are from the period 2000-2010.

Farther to the west around the Karelian Isthmus and the Gulf of Finland to Estonia, geodynamic strain lines match the 2007 earthquake fault plane. Taking into account the shallow focal depth, it is possible that there is a similarity of the GPS-measured strain rates with those derived from seismic data for the upper 3 km of the crust. The Anjalankoski 2003 swarm focal mechanisms revealed a stress–strain state that better reflects local geology. Nevertheless, the strike of the fault plane is in agreement with the GPS strain data. The EW dilatation shown in the map probably indicates recent geodynamic activity along faults transverse to the stretch of the Gulf of Finland and suggest the existence of the Narva–Anjalankoski zone.

Kaliningrad region

The Kaliningrad earthquake sequence (21 September 2004) consisted of three events. The first two were the largest (see Table 2). Gregersen *et al.* (2007) presented intensity data from Poland, Sweden, Denmark, Norway, Russia, and Finland. The intensity maps constructed from these data depict a NW–SE orientation of the EMS–98 intensity boundaries III, IV, and V. These intensity values are related to specific amplitudes of ground motion, notably surface displacements. Gregersen *et*

Table 2 Earthquake parameters (Uski *et al.* 2003, 2006; Gregersen *et al.* 2007; Assinovskaya, Ovsov 2008).

Date	Origin time GMT (h m s)	Location (º)		Depth (km)	Magnitude	Region
		Lat (N)	Lon (E)			
1981 03 27	22:00:42	61.98	29.75	10	2.1 M_L	Kesälahti
2003 05 09	21:48:29.7	60.82	26.83	2	2.1 M_L	Ananjlankoski
2004 09 21	11:05:04.6	54.85	20.04	10	5.0 M_w, 4.7 *mb*, 4.8 M_L	Kaliningrad
2004 09 21	13:32:30.8	54.88	20.05	10	5.2 M_w, 4.8*mb*, 5.0 M_L	Kaliningrad
2007 07 11	15:45:27.9	60.10	28.84	2.9	2.0 M_L	Gulf of Finland

al. (2007) also described the focal mechanisms (see Table 3) for these two earthquakes determined from centroid moment tensors with source parameters for the seismic moment of 5.0×10^{16} and 7.2×10^{16} N-m, and average displacements of 38.0 cm and 57.1 cm, for the first and second shocks, respectively. Both earthquake epicentre zones were located in the northwest part of the Sambian Peninsula. The most probable active fault zone trended N–S within a few km of the western Sambian coast (Suveizdis 2003; Assinovskaya, Ovsov 2008; Nikolaev 2009) (Fig. 3).

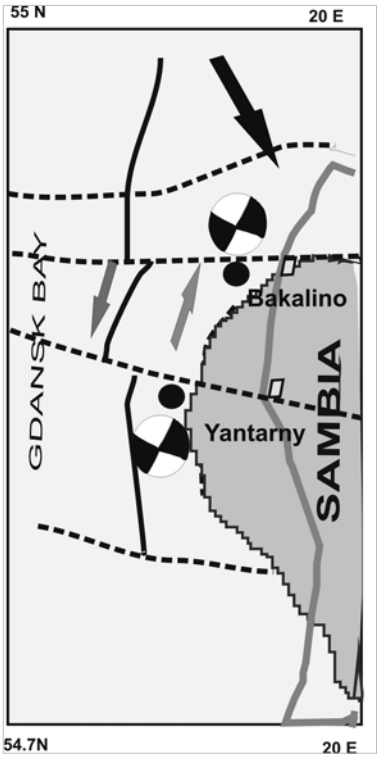

Fig. 3 Epicentre locations of the 11:05 GMT and 13:32 GMT 21 September 2004 Kaliningrad earthquakes (black circles), their focal mechanisms after Gregersen *et al.* (2007), the direction of the regional compressive stress (black arrow), the seismogenic strike–slip fault (black solid lines), its slip direction (grey arrows), and other faults of normal type (dotted lines). The grey polygon represents geological structure, probably of granitoid composition. After Assinovskaya, Ovsov (2008).

Assinovskaya, Ovsov (2008) used geophysical modeling to conclude that the N–S oriented seismogenic fault has a complex internal structure and dips under the Sambian block with the angle ~70°–80°. The first earthquake occurred at the intersection of this fault and the E–W normal fracture zone at the Yantarny settlement. The second earthquake was located at a distance of a few km to the north on the same N–S oriented fault zone near the Bakalino settlement. The focal mechanisms for these events are nearly identical and the parameters indicate strike–slip motions with a minor normal component along the possible fault planes trending E–W and N–S (see Fig. 3). The model indicates sinistral, strike–slip deformation and fracturing of the crust**.** Intensity data, source parameters, focal mechanisms, and ground motion records were used to assess co–seismic movement amplitudes in and around the earthquake site and to compare them with GPS data.

Table 3 Earthquake focal mechanism data.

Date	Fault plane	Strike (°)	Dip (°)	Reference
1981 03 27	I	171	81	Uski *et al.* 2003
	II	265	68	
2003 05 09	I	250	80	Uski *et al.* 2006
	II	70	10	
2004 09 21	I	22.00	83	Gregersen *et al.* 2007
	II	113.00	85	
2007 07 11	I	176	65	This work
	II	282	60	

Kaliningrad earthquakes co–seismic deformations

Seismically induced surface movement that can be detected by space geodetic tools requires either strong global earthquakes (M ~7–8) or seismic events located near monitoring stations. The question remains how close sensors must be stationed to record the surface motions associated with moderate seismic events such as the Kaliningrad ones. In first round analyses by Assinovskaya *et al*. (2009) and Assinovskaya, Scherbakova (2010) local and regional horizontal displacements were counted using total realized Kaliningrad earthquakes seismic moment. The data obtained were compared with the Baltic GPS observations only a month before and after the earthquakes on 21 September 2004. GPS regional horizontal displacements obtained by means of daily position and baseline data analysis have revealed co–seismic anomalies. However, they did not seem to be statistically reliable and therefore longer series of observations are now used.

In this study, seismic strong motion parameters are applied together with seismic source data and GPS data to further investigate local geodynamic motions from moderate earthquakes. Near–field and remote earthquake stress–strain data were analysed using COULOMB 3.1 and GRID_STRAIN software. Initial conditions included focal mechanism data, cumulative seismic moment, and a hypocentre depth of 10 km. From these analyses co–seismic horizontal displacement maps were constructed. A horizontal motion of about 1 m along the fault was observed in the near field. This motion decreased to 0.5–1.0 mm at a distance of nearly 70 km (the WLAD GPS station). The point far–field displacements (from ~20 km to 550 km) were determined from broadband records observed at seismograph stations around the epicentres of the Kaliningrad earthquakes and in some other places (Gregersen *et al.* 2007) by using known relations between intensity and ground motions (Ambraseys *et al.* 1996; Aptikaev *et al*. 2008).

Displacement anomalies of each station's GPS position were found as a step or impulse of the moment of the Kaliningrad earthquakes, as mentioned above. The final GPS displacements are presented in comparison with seismological data in Table 4. The absolute values of the GPS horizontal offsets are similar to those obtained from seismic data. The map of horizontal displacements in the near–field zone was compiled using earthquake focal mechanism data and is shown

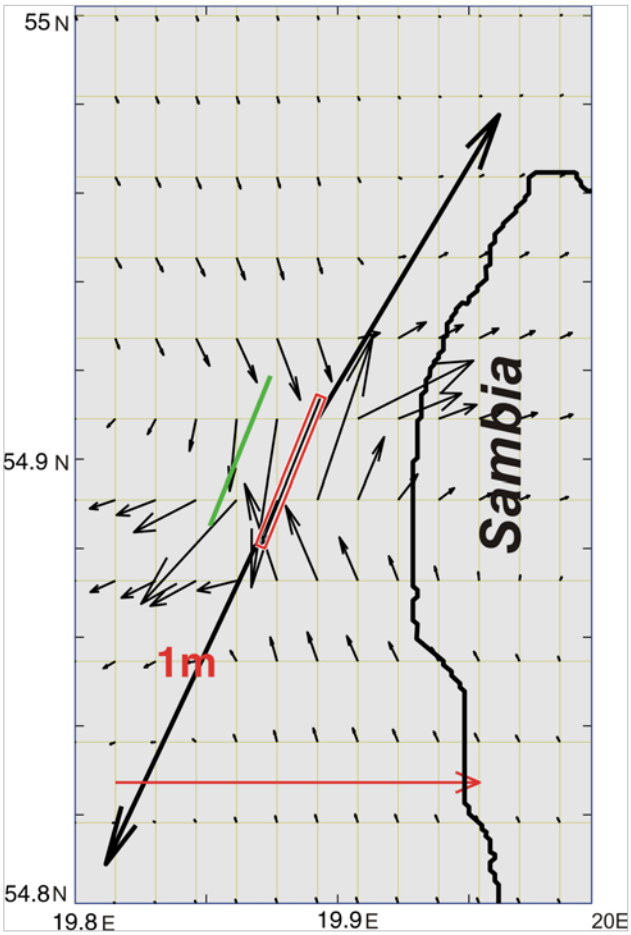

Fig. 4 Near–field co–seismic horizontal displacement for the 21 September 2004 Kaliningrad earthquakes. Black arrows represent displacement, the red line the active fault, and the green line the fault projection on the surface.

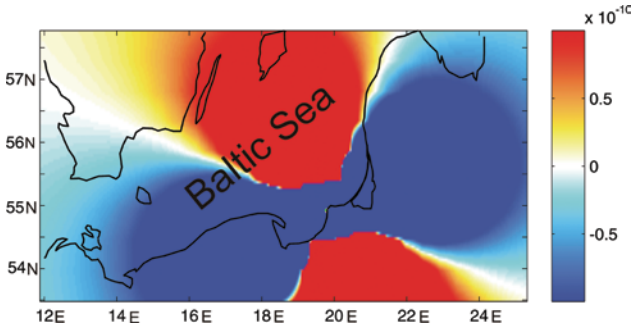

Fig. 5 Far–field co–seismic strain for the 21 September 2004 Kaliningrad earthquakes derived from focal mechanism data. Red lobes denote compression (dilatation is negative) and blue lobes dilatation (dilatation is positive).

in Fig. 4. It is seen that the maximum displacement occurred in the north–east direction. Unfortunately, there was no GPS station in the near field when the Kaliningrad earthquakes occurred.

Two maps for far–field strain zones were also generated; one using focal mechanism parameters and the other GPS results (Table 4). The seismic strain map (Fig. 5) shows co–seismic compressive and tensile deformations spread widely throughout the region as well as perceptible deformation of crust sections near the earthquake epicentres (Gregersen *et al.* 2007). The two far–field strain maps clearly represent the well-known regional NW–NE direction of compressive strain (stress) (Heidbach *et al.* 2008).

A map of the co–seismic strain pattern (Fig. 6) implies that after the earthquake the crustal deformation varied from one region to another. The central, northwestern, and eastern regions have similar horizontal

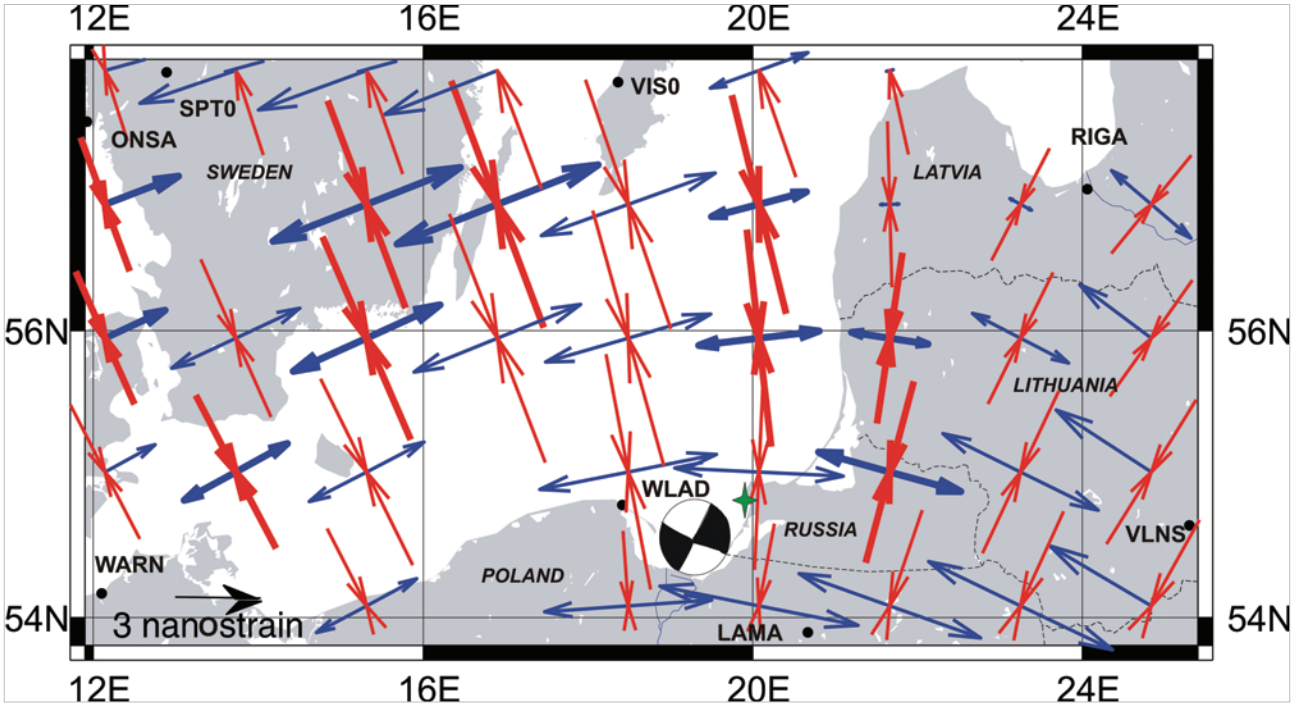

Fig. 6 The co–seismic strain field (ΔL/L, nanostrain/yr) for the 21 September 2004 Kaliningrad earthquakes. Blue arrows represent extension and red arrows compression. Arrows are scaled to strain rate. High significance is marked by bold arrows and mean significance by thin arrows in accordance with the above mentioned GRID_STRAIN software implementation.

Table 4 Horizontal displacements with errors (1-σ) on September 21, 2004 estimated by GPS and earthquake analyses. Earthquake strong motion data are from broadband seismograms, if available, or evaluated from intensity values according to Gregersen *et al.* (2007).

GPS				Earthquake	
Station	Displacement to east, mm	Displacement to north, mm	Horizontal displacement, mm	Horizontal displacement, mm	Intensity
LAMA	0.4±0.3	0.6±0.3	0.7 ±0.4	0.6	IV-V
WLAD	-1.5±0.2	1.6±0.4	2.2 ±0.4	2.5	V?
ONSA	-0.5±0.3	-0.6±0.3	0.8 ±0.4	0.5	III-IV
SPT0	-0.6±0.3	-0.5±0.3	0.8 ±0.4	0.5	III-IV
VIS0	0.6±0.2	-0.1±0.3	0.6 ±0.3	0.5	III-IV
VLNS	0.6±0.4	-0.6±0.7	0.8 ±0.8	0.3	III
RIGA	-0.4±0.3	0.1±0.4	0.6 ±0.5	0.5	III-IV
WARN	-0.5±0.3	-0.4±0.3	0.6 ±0.4	0	II

strains. Everywhere, the magnitude of the axis of maximum compression is about equal to the magnitude of the axis of maximum dilatation, but their orientations are different and vary from NW–NE to NE–SW (Fig. 6). It is notable that in the central part, to which the epicenter area belongs, the N–S strain direction coincides with the strike of the seismogenic faults. There is a potential for seismic activity along the entire length of the fault zone. Thus, GPS data combined with even moderate magnitude earthquake source data yield additional information about the regional tectonic stress and strain pattern.

CONCLUSIONS

Using permanent and field GPS station data, regional crust velocities and displacements were calculated and the strain field was mapped for two areas of the Baltic Sea region. The strain field is very heterogeneous in the Lake Ladoga–Gulf of Finland region. The strike of the dilatation zone is coincident with the ancient Lake Ladoga–Bothnian Bay suture zone (Gaal 1982). The recent seismic activity of this zone has been described by Assinovskaya, Novozhilova (2002). The Kesälahti earthquake cluster located here may be associated with the regional dilatational stress; at least the focal mechanisms for this region do not preclude such a hypothesis. On the other hand, the data are too sparse to conclude this for sure.

In the region of the Gulf of Finland, strain data obtained by GPS do not contradict focal mechanism solutions. The earthquake fault planes occurred in the direction of maximum strain, implying that the upper 3 km of the crust have experienced recent deformation. The well constrained source mechanism of the 21 September 2004 Kaliningrad earthquakes leads to a greater understanding of the geodynamics throughout the Eastern Baltic. Stress–strain field modelling based upon focal mechanisms from these earthquakes is in general agreement with the post–seismic geodynamical deformation observed by GPS–based ground movement.

Thus, the geodynamic activity is expressed by the presence of both long–term and short–term alternating regional movements and wherever non-uniform GPS local motions occur. This crust mobility may be responsible for the earthquake occurrence that in turn forms abnormal ground movements recorded both in seismic and geodynamic data.

Acknowledgements

The study was partly funded by the Saint Petersburg Scientific Centre of the Russian Academy of Sciences (SPbRC RAS) 2006–2010 Scientific Programme. The authors are grateful to reviewers especially to Dr. Tom Shoberg (Rolla, Missouri) for helpful comments that allowed improvements to be made to the quality of the manuscript and the interpretation of results, and to Dr. Valerijs Nikulins (Rīga) for his positive opinion. The special thank is given to Dr. Rutger Wahlström (GeoForschungsZentrum, Potsdam). The authors are thankful to Dr. J.-P. Boy (Greenbelt, Maryland) for the calculation of the hydrological loading effect of lakes Ladoga and Onega and to colleagues for the original GPS data placed at our disposal.

References

Ahjos, T., Uski, M., 1992. Earthquakes in northern Europe in 1375–1989. *Tectonophysics 207,* 1–23.

Altimeter data, 2010. Web source: http://www.pecad.fas.usda.gov/cropexplorer/

Amantov, A.V., Zhamoida, V.A., Manuilov, S.F., Moskalenko, P.E., Spiridonov, M.A., 2002. Geology and mineral recources of the Eastern Gulf of Finland. *Regional geology and metallogeny 15,* VSEGEI, 120–133. [In Russian].

Ambraseys, N.N., Simpson, K.A., Bommer, J.J., 1996. Prediction of horizontal response spectra in Europe. *Earthquake Engineering and Structural Dynamics 25 (4),* 371–400.

Aptikaev, F., Borcia, I. S., Erteleva, O., Sandi, H., Alcaz, V., 2008. Development of instrumental criteria for intensity estimate. Some studies performed in the frame of a NATO Project. *Constructii 6 (2),* 18–25.

Assinovskaya, B.A., 2005. Seismic events on Lake Ladoga in the XX century. *News of Russian Geographical Society 1379 (4),* 70–76. [In Russian].

Assinovskaya, B.A., Novozhilova, T.V., 2002. On the question of the seismic hazard level in the St. Petersburg region. *Proceedings of the Central Astronomical Observatory of the Russian Academy of Sciences at Pulkovo 216*, 394–401. [In Russian].

Assinovskaya, B.A.,Verzilin, N.N., 2007. On the seismic hazard in the Baltic Sea. *Proceedings of International Conference "The changing geological environment: spatiotemporal interaction of endogenous and exogenous processes",* Kazan', November 12–16, 2007, 210–213. [In Russian].

Assinovskaya, B. A., Ovsov, M. K., 2008. Seismotectonic position of the Kaliningrad September 21, 2004 earthquake. *Izvestiya Physics of the Solid Earth 44 (9),* 717–727. [In Russian].

Assinovskaya, B.A., Malkin, Z. A., Scherbakova, N.V., 2009. Connection of surface and deep geodynamics for example of Kaliningrad earthquake September 21, 2004. *Proceedings of Central Astronomical Observatory of the Russian Academy of Sciences at Pulkovo 219 (4),* 33–39. [In Russian].

Assinovskaya, B.A., Scherbakova, N. V., 2010. Seismodynamics of Kaliningrad September 21 2004 earthquake. *Proceedings of XVI Internationa l Conference "East–European Platform lithosphere structure, properties, dynamics and minerageny, September 20–25, Voronezh,* 86–89. [In Russian].

Avotinia, I.Y., Boborikin, A.M., Yemelianov, A.P., Sildvee, X.X., 1998. Catalogue of historical earthquakes of Belarus and the Baltic Region. *Seismological report of seismic stations of Minsk–Pleshchenitsi and Naroch for 1984*, Minsk, 126–137. [In Russian].COULOMB 3.1 software, 2010. Web source: http://earthquake.usgs.gov/research/modeling/coulomb

FENCAT database, 2010.Web source: http://www.seismo.helsinki.fi

Fjeldskaar, W., Lindholm, C., John, F., Dehls, J.F., Fjeldskaar, I., 2000. Postglacial uplift, neotectonics and seismicity in Fennoscandia. *Quaternary Science Reviews 19 (14–15),* 1413–1422.

Gaal, G., 1982. Proterozoic tectonic evolution and late Svecokarelian plate deformation of the Central Baltic Shield. *Geologische Rundschau 71(1), 158–170.*

GPS archive, 2010. Source: ftp://garner.ucsd.edu/pub/rinex/; ftp://cddis.gsfc.nasa.gov/pub/gps/ data/daily/

Gregersen, S., Wiejacz, P., Debski, W., Domanski, B., Assinovskaya, B., Guterch, B., Mäntyniemi, P., Nikulin, V.G., Pacesa, A., Puura, V., Aronov, A.G., Aronova, T.I., Grunthal, G., Husebye, E.S., Sliaupa, S., 2007. The exceptional earthquakes in Kaliningrad District, Russia on September 21, 2004. *Physics of the Earth and Planetary Interiors 164 (1–2)*, 63–74.

Gruntal, G., Stromeyer, D, Wylegalla, K, Kind, R., Wahlstrom, R., Yuan, X., Bock, G The M_w 3.1-4.7 earthquakes in the southern Baltic Sea and adjacent areas in 2000, 2001 and 2004. 2008. *Seismology 12, 3,* 413-429.

Heidbach, O., Tingay, M., Barth, A., Reinecker, J., Kurfeß, D., Müller, B., 2008.The World Stress Map database, release 2008. Web source: http://dc-app3-14.gfz-Potsdam.de/pub/ release_2008/ release_2008.html

Karpinsky, V.V., Assinovskaya, B.A., Gorshkov, V.L., Ivanov, V.Yu., 2006. Seismic station Valaam. *Proceedings of the Central Astronomical Observatory of the Russian Academy of Sciences at Pulkovo 218,* 216–220. [In Russian].

Lidberg, M., Johansson, J. M., Scherneck, H.-G., Milned, G. A., 2010. Recent results based on continuous GPS observations of the GIA process in Fennoscandia from BIFROST. *Journal of Geodynamics 50,* 8–18.

Lin, J., Stein, R.S., 2004. Stress triggering in thrust and subduction earthquakes, and stress interaction between the southern San Andreas and nearby thrust and strike-slip faults. *Journal of Geophysical Research 109, B02303.* doi:10.1029/2003JB002607.

Nikolaev, A.V. (editor), 2009. *Kaliningrad earthquake September 21, 2004.* A. P. Karpinsky Russian Geological Research Institute, Saint-Petersburg, 170 pp. [In Russian].

Nikonov, A.A., 2005. The Eastern Ladoga earthquake November 30, 1921. *Physics of the Earth 7,* 1–5. [In Russian].

Nikonov, A.A., 2006. About the mechanism of September 21, 2004 Kaliningrad earthquake source. *Doklady RAN 407, 1.* 102-105. [In Russian].

Pagaczewski, J., 1972. Catalogue of earthquakes in Poland in 1000–1970 years. *Publications, Institute Geophysics Poland Academy of Science 51,* 3–36**.**

Pascal, C., Stewart, I.S., Vermeersen, B.L.A., 2010. Neotectonics, seismicity and stress in glaciated regions March. *Journal of the Geological Society 167,* 361–362.

Petrov, L., Boy, J.-P., 2004. Study of the atmospheric pressure loading signal in VLBI observations. *Journal of Geophysical Research 10, 109,* B03405. Web source: http://gemini.gsfc.nasa.gov/ aplo

Renquist, H., 1931. *Finlands jordskalv 1931*. Fennia 54 (1), 113 pp.

Scherbakova, N.V., Gorshkov, V.L., 2007. Dynamic of mutual position of North-West Europe GPS net. *Geodesy and Cartography 11,* 15–18. [In Russian].

Scherneck, H.-G., Lidberg, M, Haas, R., Johansson, Jan M., Milne, G.A., 2010. Fennoscandian strain rates from

BIFROST GPS: A gravitating, thick-plate approach. *Journal of Geodynamics 50 (1)*, 19–26.

Suveizdis, P. (Ed.), 2003. *Tectonic map of Lithuania. 1: 500 000.* Institute of Geology and Geography, Vilnius.

Teza, G., Pesci, A. Galgaro, A., 2008**.** Grid_strain and grid_strain3: Software packages for strain field computation in 2D and 3D environments. *Computers & Geosciences 34,* 1142–1153.

Toda, S., Stein, S. R., Richards-Dinger, K., Bozkurt, S., 2005. Forecasting the evolution of seismicity in southern California: Animations built on earthquake stress transfer. *Journal of Geophysical Research 110, B05S16.* doi:10.1029/2004JB003415.

Uski, M., Tiira, T., Korja, A., Elo, S., 2006. The 2003 earthquake swarm in Anjalankoski, south–eastern Finland. *Tectonophysics 422 (1–4),* 55–69.

Uski, M., Hyvonen, T., Korja, A., Airo, M.-L., 2003. Focal mechanisms of three earthquakes in Finland and their relation to surface faults. *Tectonophysics 363,* 141–157.

Wdowinski, S., Bock, Y., Zhang J., Fang, P., Genrich J., 1997. Southern California Permanent GPS Geodetic Array: Spatial filtering of daily positions for estimating coseismic and postseismic displacements induced by the 1992 Landers earthquake. *Journal of Geophysical Research 102, B8.* 18,057-18,070.

Wiejacz, P., 2004. Preliminary investigation of the September 21, 2004 earthquakes of Kaliningrad Region, Russia. *Acta Geophysica Polonica 52,* 425–441.

Wu, P., Johnston, P., Lambeck, K., 1999. Postglacial rebound and fault instability in Fennoscandia. *Geophysical Journal International 139,* 657–670.